Received: 27 September 2018 | Revised: 18 January 2019 | Accepted: 21 January 2019

DOI: 10.1111/vop.12651

ORIGINAL ARTICLE

WILEY

Morphological and immunohistochemical characteristics of the equine corneal epithelium

Eva Kammergruber[1] | Carolin Rahn[1] | Barbara Nell[2] | Simone Gabner[1] | Monika Egerbacher[1]

[1]Histology and Embryology, Department of Pathobiology, University of Veterinary Medicine, Vienna, Austria

[2]Department of Companion Animals and Horses, University of Veterinary Medicine, Vienna, Austria

Correspondence
Simone Gabner, Histology and Embryology, Department of Pathobiology, University of Veterinary Medicine, Vienna, Austria
Email: simone.gabner@vetmeduni.ac.at

Present Address
Eva Kammergruber, Department of Pathobiology, Faculty of Veterinary Medicine, Utrecht University, Utrecht, The Netherlands

Carolin Rahn, AstraZeneca Austria, Vienna, Austria

Abstract

Objective: The morphology of the corneal epithelium in two age groups of horses is described. Distribution patterns of proliferation-, differentiation-, stem cell-associated markers and cell junction proteins were assessed.

Methods: Corneal samples from 12 horses (six foals and six adult horses) were analyzed after H&E staining and immunohistochemistry using the following antibodies: E-cadherin, β-catenin, Connexin 43 (Cx43), tight junction protein 1 (TJP1), cytokeratin (CK) 14, CK 19, CK 3, CK 10, vimentin, Ki67, p63, nerve growth factor (NGF), ABCG2, and epithelial growth factor receptor. Semiquantitative analysis of crypt, limbal, peripheral, and central zone was performed. Semithin and ultrathin sections were used for ultrastructural evaluation of the epithelium.

Results: The height of the epithelium varied between age groups and crypts were consistently present. In the peripheral and central epithelium, three types of basal cells resembling a pseudostratified epithelium were characterized. Potential stem cell markers (CK 14, p63, NGF, and ABCG2) were present in all zones with decreasing frequency toward the center. Cornea-specific differentiation marker CK 3 was not expressed in the most basal cell layer of the limbal epithelium. E-cadherin, β-catenin, and Cx43 revealed a similar apico-lateral signal pattern throughout the entire epithelium; only TJP1 was additionally seen at the basal surface.

Conclusions: This study presents a systematic semiquantitative evaluation of the equine corneal epithelium, showing the presence of crypts as potential stem cell niche with CK 14, p63, NGF, and ABCG2 as relevant markers for cells with regenerative capacity. The pseudostratified arrangement of the basal layer was a unique finding.

KEYWORDS

cell junction proteins, corneal stem cell niche, crypt, horse, limbus, semiquantitative evaluation

This is an open access article under the terms of the Creative Commons Attribution-NonCommercial-NoDerivs License, which permits use and distribution in any medium, provided the original work is properly cited, the use is non-commercial and no modifications or adaptations are made.
© 2019 The Authors. *Veterinary Ophthalmology* published by Wiley Periodicals, Inc. on behalf of American College of Veterinary Ophthalmologists

1 | INTRODUCTION

For the corneal epithelium, differences have been reported in various mammals regarding micromorphological architecture and stem cell localizations.[1,2] In the horse, conflicting statements concerning the components of the corneo-scleral junction, commonly called limbus, as well as the structure of the actual corneal epithelium have been made. Crypts or crypt-like structures have been postulated both to be present and lacking.[3,7] For the equine corneal epithelium Nautscher et al[5] described three layers: a *stratum superficiale*, a *stratum intermedium,* and a *stratum basale*. In contrast, Ledbetter and Scarlett[9] divided the equine epithelium into four layers: a superficial, a superficial-intermediate (wing cells), a deep intermediate, and a basal cell layer. The Bowman's layer, which is described for the cornea of humans and primates, is not present in the equine cornea.[5,9]

Intercellular junctional complexes are required for an intact cornea epithelial barrier as well as for intraepithelial cell communication and have therefore been studied in healthy and diseased corneas of various species.[10,11] Several types of cell junctions are known which can functionally be grouped into adhering, occluding, and communicating junctions composed of proteins like E-cadherin, β-catenin, tight junction protein1 (TJP1, also known as zonula occludens1, ZO1), and connexin 43 (Cx43).

In corneal epithelium, the maintenance and regeneration of cell mass is thought to be primarily achieved by a distinct population of stem cells (SCs). In humans, four microanatomical structures have been described as corneal stem cell niches at the corneo-scleral junction: Palisades of Vogt, limbal epithelial crypts, limbal crypts, and focal stromal projections.[11,14,15] It was further hypothesized, that corneal epithelial SCs are distributed over the entire corneal surface, since acute corneal wounds can be repaired without the influence of limbal SCs.[17] Data about localizations of potential stem cell niches and their identification are sparsely available in veterinary ophthalmology.[6]

As there is no current consensus about distinct species-specific markers to detect SCs and their subsequent differentiation stages (eg, transient amplifying cells, TACs) in the cornea, only a combination of differentiation, and putative SC-associated markers can provide a suitable approach for identifications of SCs.[11,18] Cytokeratin (CK) proteins belong to the intermediate filament family of cytoskeletal proteins and contribute crucially to the maintenance of cell structure and intercellular adhesion.[19] Cytokeratins are valuable diagnostic makers, as their changes are associated with epithelial cell differentiation, response to epithelial injury and epithelial regeneration.[20] In humans, p63, nerve growth factor (NGF), ABCG2 and higher expression levels of epithelial growth factor receptor (EGFR) have been reported to be positive markers for the detection of corneal SCs.[18,21,22] So far, only p63 has been studied in the equine cornea and positive cells have been detected in the limbus and the crypt-like structure.[3,7]

The aim of this study was to analyze the structure of the equine corneal epithelium including the corneo-scleral junction using light- and electron microscopy. We furthermore systematically explored the distribution of cell junction proteins (E-cadherin, β-catenin, Cx43, and TJP1), as well as markers for cell differentiation (cytokeratins, vimentin) and cell renewal (Ki67), including identification of potential SC markers (p63, NGF, ABCG2, and EGFR).

2 | MATERIALS AND METHODS

2.1 | Animals and tissue preparation

Corneal samples from 12 horses, which were divided into two age groups representing foals and adult horses were collected between 2-12 hours after euthanasia (Table 1). Horses were euthanized due to reasons unrelated to this study and had no ocular diseases confirmed by a board-certified ophthalmologist. Written consent for tissue sampling and work up was given upon agreement to euthanasia by the owners.

After in toto removal of corneas from the globes including the corneo-scleral junction, the right and left cornea of each horse were randomly chosen to be cut in half in either dorso-ventral (DV) or naso-temporal (NT) direction. Samples were fixed in either 4% buffered formalin or methacarn (methanol-chloroform-acetic acid at a volume ratio of 6:3:1) for 24-48 hours at room temperature. Afterward, a strip of 5 mm width extending from one cornea-scleral junction via the center to the contra-lateral junction (Figure 1A) was embedded in paraffin (HistoComp, Sanova, Vienna, Austria) via an automated embedding system

TABLE 1 Animals used

Individual	Breed	Sex	Age
Foal 1	Quarter horse	s	2 d
Foal 2	Shetland pony	s	9 mo developed fetus
Foal 3	Icelandic pony	m	18 d
Foal 4	Warmblood	s	6 d
Foal 5	Quarter horse	s	3 d
Foal 6	Shetland pony	m	1 mo
Adult 1	Holsteiner	g	20 y
Adult 2	Haflinger	g	4 y
Adult 3	Tinker	m	10 y
Adult 4	Trotter	g	26 y
Adult 5	unknown	m	11 y
Adult 6	Trotter	g	21 y

g, gelding; m, mare; s, stallion.

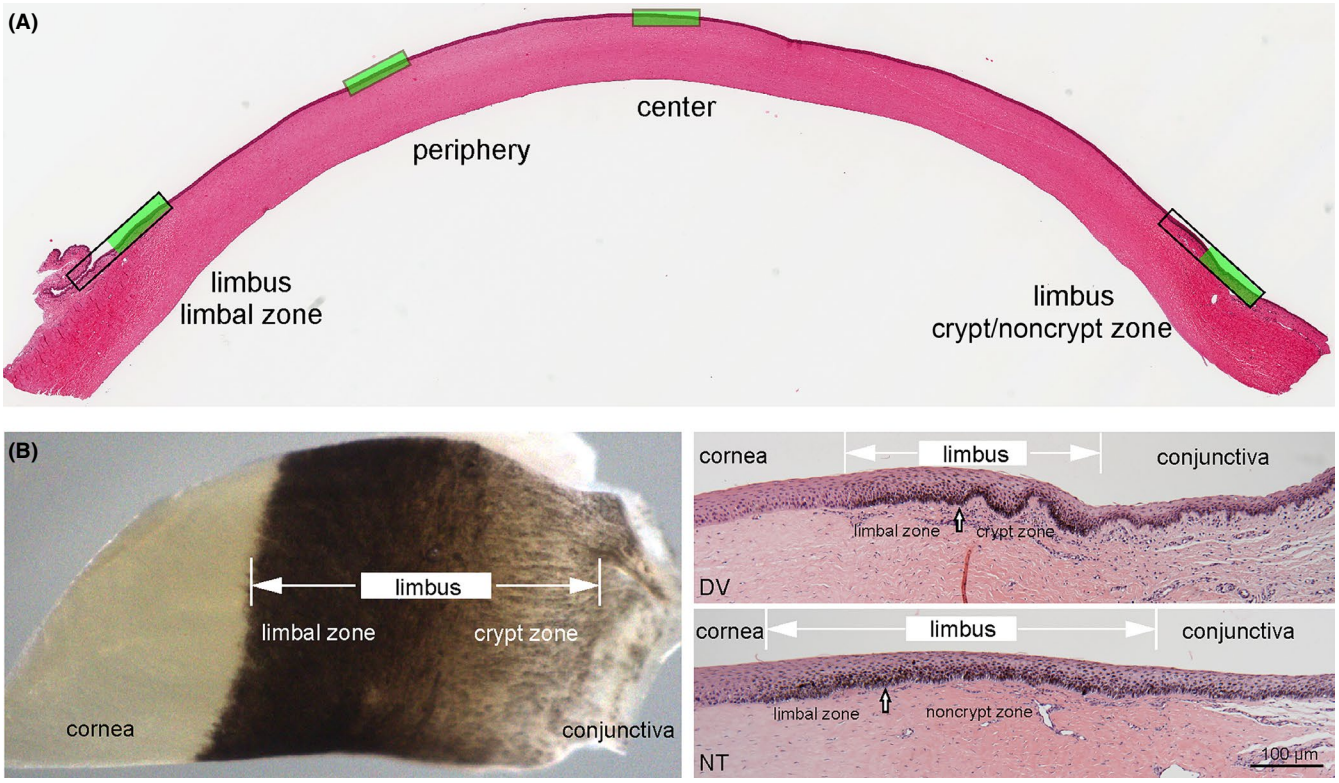

FIGURE 1 Morphology of the equine cornea: overview of an entire cornea cross section with the four examined zones marked in green (A). Picture of a whole mount sample of the transitional zone from cornea to conjunctiva, clearly depicting two distinct subzones in the limbus and cross sections of these zones, showing crypts in dorso-ventral (DV) sections and noncrypt zone in naso-temporal (NT) sections (B). Note differences in the composition of the underlying stroma including vasculature which is distinctive in the different zones. Scale bar =100 µm

(Shandon–Excelsior, Histocom, Wiener Neudorf, Austria). Serial sections of 4 µm were mounted on APES- (3-aminopropyltriethoxy-silane/glutaraldehyde) coated slides.

For electron microscopy, 1-2 mm^3 pieces of the central cornea were fixed with 3% buffered glutaraldehyde (Carl Roth GmbH, Karlsruhe, Germany) and stored at 4°C until further processing. After rinsing with Sœrensen's phosphate buffer 0.1 mol/L, pH: 7.4, samples were postfixed in 1% OsO_4 (Electron Microscopy Sciences, Hatfield, PA) for 2 hours at room temperature. Washing with phosphate buffer followed, and dehydration was performed in a series of graded ethanol solutions. Embedding with propylene oxide was performed by increasing ratios of epoxy resin-propylene oxide (1:1, 3:1) and finally pure resin (Serva, Mannheim, Germany). After two additional changes, the resin was polymerized for 48 hours at 60°C. Semithin (1 µm) and ultrathin (70 nm) transverse sections were cut using an ultramicrotome (Reichert Ultracut S, Leica, Vienna, Austria). The sections were mounted on copper grids (Gröpl, Tulln, Austria) and stained with uranyl acetate and lead citrate (Sigma-Aldrich, Steinheim, Germany).

2.2 | Histology and immunohistochemistry

Microstructure of the corneal epithelium and the corneoscleral junction (particularly the existence of crypts in the limbus) were assessed after Hematoxylin and Eosin (H&E) staining. Furthermore, epithelial thickness was measured using a Nikon Imaging Software (NIS-Elements D 3.2) in micrographs of peripheral and central cornea in both DV and NT direction. Of every examined zone, two micrographs (ie, eight micrographs per horse) were taken and in every micrograph three measurements were performed. For statistical analysis of epithelial thickness, age groups were compared using mixed models. In addition, the number of epithelial cell layers was counted in the center of the cornea.

For immunohistochemistry, endogenous peroxidase activity was blocked by incubation in 0.6% H_2O_2 in methanol for 15 minutes at room temperature. A protein block (1.5% normal goat serum) was used to minimize unspecific binding of the primary antibody. For sources, pretreatments and dilutions of the respective primary antibodies used in this study see Table 2. HistoGreen/Histoprime® (Linaris Biologische Produkte GmbH, Wertheim–Bettingen, Germany) was used as secondary detection system. Finally, slides were washed with distilled water, counterstained with Nuclear Fast Red solution (Sigma-Aldrich, St. Louis, MO) dehydrated and mounted using a xylene-soluble medium (DPX, Fluka, Buchs, Switzerland).

For fluorescent detection of primary antibodies, Alexa Fluor™ 568 or 488 goat anti-mouse/rabbit secondary

TABLE 2 Sources, dilutions, fixations and pretreatments of the antibodies used

Antibody	Function	Clone	Host	Source	Dilution	Fixation	Pretreatment
E-cadherin	Adhering cell junction	Polyclonal	Rabbit	Santa Cruz, CA, USA	1:150	f	Tris-EDTA buffer pH 9.0, 30 min steamer
β-catenin	Adhering cell junction	9G2	Mouse	Acris, Herford, Germany	1:100	f	Tris-EDTA buffer pH 9.0, 30 min steamer
Cx43	Communicating cell junction	Polyclonal	Rabbit	Sigma, MO, USA	1:2000	f	0.1% Protease (Sigma) in PBS, 20 min at RT
TJP1	Occluding cell junction	Polyclonal	Rabbit	Sigma Prestige, MO, USA	1:200	f	Tris-EDTA buffer pH 9.0, 30 min steamer
CK 14	Cytoskeleton, cell differentiation	LL002	Mouse	Leica Biosystems, Newcastle, UK	1:100	m	Tris-EDTA buffer pH 9.0, 20 min steamer
CK 19	Cytoskeleton, cell differentiation	Polyclonal	Rabbit	Bioss, MA, USA	1:500	m	No pretreatment
CK 3	Cytoskeleton, cell differentiation	AE5	Mouse	Merck Millipore, MA, USA	1:100	f	0.01 mol/L citrate buffer pH 6.0, 30 min steamer
CK 10	Cytoskeleton, cell differentiation	LH2	Mouse	Santa Cruz, CA, USA	1:100	f	0.01 mol/L citrate buffer pH 6.0, 30 min steamer
Vimentin	Cytoskeleton, cell differentiation	V9	Mouse	Dako, CA, USA	1:200	m	0.01 mol/L citrate buffer pH 6.0, 30 min steamer
Ki67	Cell proliferation	8D5	Mouse	Cell Signaling Technology, MA, USA	1:200	f	0.01 mol/L citrate buffer pH 6.0, 30 min steamer
p63	Potential SC marker	Polyclonal orb214808	Rabbit	Biorbyt, Cambridge, UK	1:2500	f	0.01 mol/L citrate buffer pH 6.0, 30 min steamer
NGF	Potential SC marker	E-12	Mouse	Santa Cruz, CA, USA	1:100	f	0.01 mol/L citrate buffer pH 6.0, 30 min steamer
ABCG2	Potential SC marker	B-1	Mouse	Santa Cruz, CA, USA	1:100	m	Tris-EDTA buffer pH 9.0, 30 min steamer
EGFR	Potential SC marker	A10	Mouse	Santa Cruz, CA, USA	1:200	m	Tris-EDTA buffer pH 9.0, 30 min steamer

f, formol; m, methacarn; PBS, phosphate-buffered saline; RT, room temperature.

antibodies (Molecular Probes, Carlsbad, CA; dilution 1:100 in phosphate buffered saline) were used and nuclear counterstaining was performed with 4′,6-diamidino-2-phenylindole (DAPI, Molecular Probes). Negative controls were performed by substitution of the primary antibodies with phosphate buffered saline to demonstrate the specificity of the secondary system. Sections of equine intestine, skin, heart, and brain were used as positive controls.

Paraffin and semithin sections were examined via light microscopy (DM 2000, Leica) and images were captured using a DFC 425 C digital camera system (Leica). Fluorescence images were analyzed and captured with a LSM 880 confocal laser scanning microscope (Zeiss, Oberkochen, Germany). Ultrathin sections were examined and transmission electron micrographs were taken using the transmission electron microscope EM900 (Zeiss) at a 50 000 magnification with a digital Frame Transfer CCD camera (Tröndle TRS, Moorenweis, Germany) using SiS software (ImageSP Professional, Tröndle TRS).

2.3 | Evaluation of immunohistochemistry

For semiquantitative evaluation of immunohistochemistry crypts and noncrypts (pigmented zone with or without epithelial undulations at the transition of limbus to conjunctiva), limbus (pigmented zone between crypts and cornea without epithelial undulations), periphery (half way between limbus and center) and center (Figure 1A). In each zone, one high-power field (HPF) at 40x magnification was used and the whole thickness of the epithelium was evaluated. A scoring system ranging from 0-4 was applied representing all positively stained cells per HPF on a percentage basis: 0% (score 0), 1%-33% (score 1), 34%-67% (score 2), 68%-99% (score 3) and 100% (score 4). For statistical analysis, age groups were

compared using Mann-Whitney U tests. Differences between zones were analyzed using nonparametric Friedman tests followed by Wilcoxon tests with Bonferroni´s α-correction procedure as post hoc comparisons. A P-value <0.05 was assumed as significant.

3 | RESULTS

3.1 | Histology

The analysis of H&E stained corneas of foals and adult horses showed overall comparable microarchitecture. Within the pigmented corneo-scleral junction, called limbus, two distinct zones could be detected: (a) a zone of thickened epithelium continuous with the cornea with typical palisade-like basal cells (limbal zone), and adjacent (b) either a crypt zone with distinct epithelial crypts and stromal papillae (only seen in DV sections) or a noncrypt zone marked by very flat undulations (seen in NT sections) (Figure 1B). Crypts were detected in both age groups. The crypt zone appeared to be less extended in foals but was proportional to the size of the cornea. The limbus could be distinguished from the conjunctiva by arrangement of more loose connective tissue and expression of respective markers in the epithelium (Figure 1B).

In both age groups, no major difference in thickness was seen between central and peripheral epithelium in both

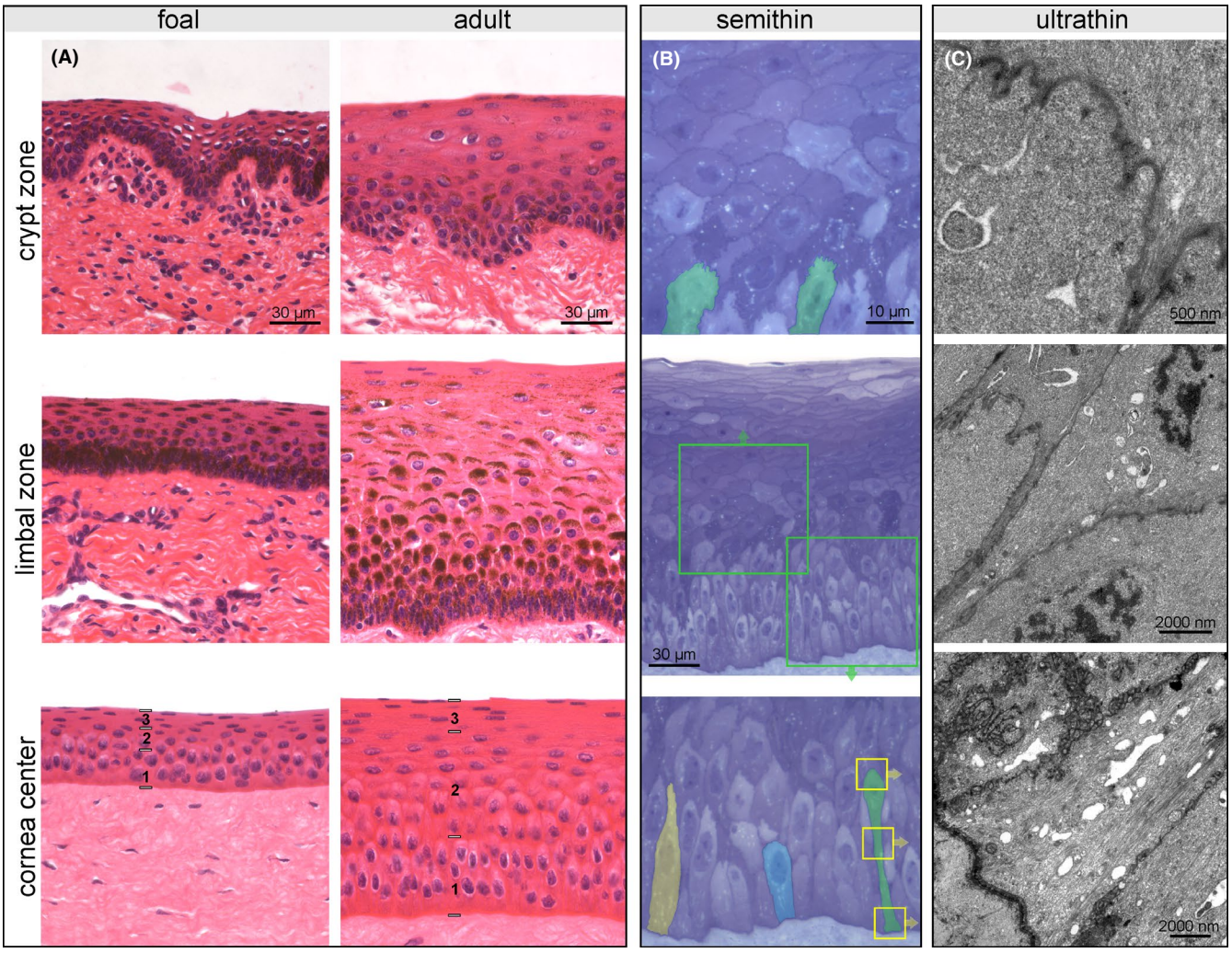

FIGURE 2 Representative pictures of crypt zone, limbal zone, and central corneal epithelium illustrating age-dependent differences (A); in the center of the cornea, a basal (1), intermediate (2), and superficial layer (3) can be distinguished. H&E staining, scale bar =30 µm. Presentation of the total corneal epithelial height (B, center image), detailed view of the intermediate layer (C, upper image) and the basal layer (C, lower image) in a semithin section from the central zone of an adult horse. Toluidine blue staining, scale bar =30 µm and 10 µm respectively. Cells in the intermediate layer have a polygonal shape with horizontal orientation, the suprabasal cell layer being in tight contact with the undulating cell border of the subjacent basal cells (examples marked in green). Three different types of basal cells form a pseudostratified basal layer (highlighted in yellow, blue and green). Cellular details of the cell highlighted in green (yellow boxes) are shown in transmission electron micrographs of ultrathin sections (C) showing the apical interdigitations as well as multiple adhering and occluding junctions at the cell membrane. Scale bar =500 nm and 2000 nm, respectively

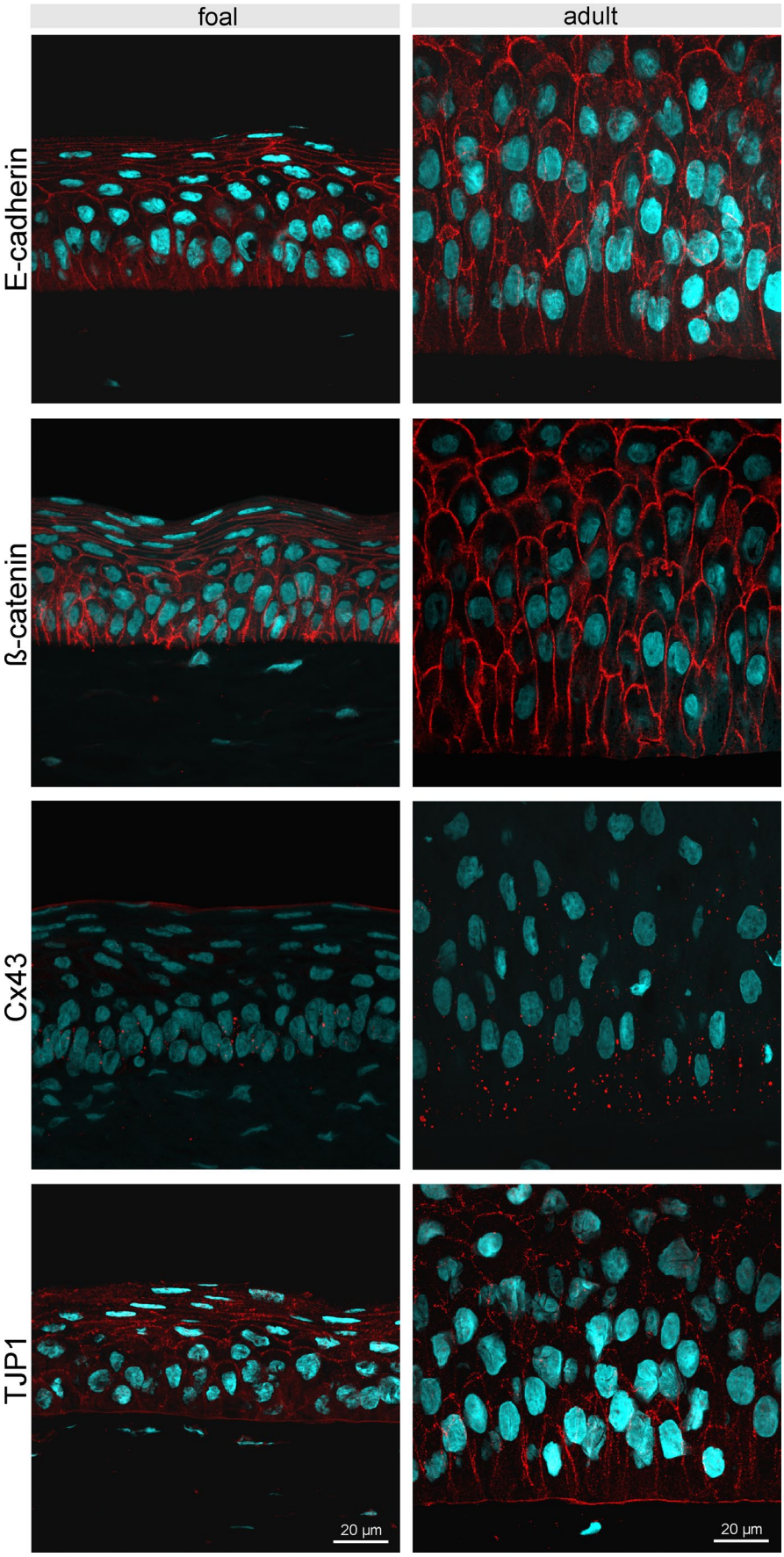

FIGURE 3 Immunofluorescent staining of E-cadherin, β-catenin, Cx43, and TJP1 of the central corneal epithelium comparing age groups (foal: left panels; adult horse: right panels). E-cadherin is expressed in the full height of the epithelium, but is not expressed at the area of contact with the basement membrane. Detection of β-catenin resembles the distribution and localization of E-cadherin expression. Cx43 is mainly present in the basal epithelial layer. TJP1 was found in all cells including the basal cell membrane. Scale bar =20 µm

DV and NT sections (Figure 1A). The epithelial height in foals compared to adult horses was significantly lower in the periphery (71.56 μm (±20.38) vs 160.61 μm (±41.09), $P < 0.001$) as well as in the center (78.06 μm (±19.07) vs 162.54 μm (±29.59), $P < 0.001$) (Figure 2A). Also, the number of cell layers was lower in foals (10.67 ± 1.56) compared to adults (17.07 ± 2.09).

Analysis of H&E stained and semithin sections revealed three distinct layers within the corneal epithelium: a superficial layer with flat cells, an intermediate layer consisting of polygonal cells with horizontal orientation and a basal layer (Figure 2A,B, center image). Suprabasal cells of the intermediate layer were in tight contact with the undulating cell border of the subjacent basal cells (Figure 2B, upper image). In adult horses only, the basal layer consisted of three recurring types of cells (Figure 2B, lower image). All of them had contact to the basement membrane but differed regarding their size and shape (Figure 2B). The shortest basal cell showed a compact exterior with its nucleus in the first row and a roundish apical compartment (illustrated as blue cell in Figure 2B). The second cell type possessed a notable apical extension with its nucleus above the basal row (illustrated as yellow cell in Figure 2B). The highest cell with the nucleus in the third, sometimes fourth row (illustrated as green cell in Figure 2B) showed a thin elongated *pedunculus* to the basement membrane which was tightly packed with cytokeratins (Figure 2C). The apical cell compartment revealed remarkable undulations of cell membrane and spots of thickened cell membrane representing cell adhesions and communications (Figure 2C).

3.2 | Immunohistochemistry

E-cadherin was expressed in the entire height of the epithelium in all examined zones, but showed less signal intensity toward the superficial cell layers, and was not expressed at the cells' contact with the basement membrane (Figure 3). Labeling of β-catenin resembled the distribution and localization of E-cadherin expression. The three basal cell types described above including their apical undulations were clearly visible in E-cadherin and β-catenin immunohistochemistry (Figure 3), since both proteins were localized at the cell membrane. Cx43 was expressed only in the basal epithelial layer but identical in all examined zones. The distribution of TJP1 showed a similar pattern to E-cadherin and β-catenin expression, with the exception that TJP1 was also present at the area of contact to the basement membrane (Figure 3). Distribution and signal intensity of the analyzed cell junction proteins did not differ between foals and adult horses.

Both CK 14 and CK 19 were expressed in all examined zones of foals and adult horses, with more stained cells and higher staining intensity within the limbus (Figures 4A,B and 5). However, we found different staining patterns for CK 14 and CK 19 in the cornea: groups of cells or single cells were distinctly positive for CK 14 in contrast to an even, but weaker staining for CK 19. Overall, foals showed more groups of CK 14 positive cells in the center of the corneal epithelium (Figure 4A). Within the limbus, cells stained positive for CK 19 in the basal cell compartment, whereas in the periphery and center the signal was located predominately in the apical cell compartment (Figure 5). Cornea-specific differentiation marker CK 3 was generally present throughout the epithelial superficial and intermediate layer, absent in the most basal layer of the entire limbus and showed decreased staining intensity in the basal layer of the peripheral and central corneal epithelium (Figures 4C and 5). Starting with few positive cells already in the conjunctiva, the signal of CK 3 increased within the crypt/noncrypt zone with some superficial cells remaining negative (Figure 5). Scattered CK 10 positive cells were detected in crypt/noncrypt and limbal zone in foals and in the limbal zone only in adult horses (Figures 4D and 5). Vimentin was detected in some basal cells of the limbus, but single positive cells were also present in the remaining two zones in adult horses and in the peripheral zone in foals (Figures 4E and 5).

Cell nuclei positive for Ki67 were observed mainly in the basal epithelial layer throughout all zones, whereas in the limbus positive nuclei were also detected in suprabasal cells, an observation that was predominately made in foals (Figures 4F and 6). The frequency of p63 positive cell nuclei decreased from the crypt/noncrypt zone toward the center in foals and adult horses and was generally higher in more superficial cell layers in foals (Figures 4G and 6). NGF showed a similar distribution and location but with weaker signal intensity than p63 (Figures 4H and 6). In the limbal zone, statistically significant more NGF positive cells ($P = 0.041$) were found in foals compared to adult horses (Figure 4H). ABCG2 was present in all examined zones in both age groups, clearly expressed by the basal epithelial cells with a cap-like staining pattern around the nucleus (Figures 4I and 6). Adult horses reached a significantly higher score of ABCG2 positive cells ($P = 0.004$) in the crypt/noncrypt zone, whereas in foals staining intensity was higher in the center of the cornea (Figures 4I and 6). Without differences between age groups, EGFR was more prominent in the limbus and showed a weaker signal in peripheral and central zones resulting in a more distinct localization at the cell membrane (Figures 4J and 6).

4 | DISCUSSION

Horses have a predisposition toward a variety of corneal disorders associated with the corneal epithelium and are affected by the most severe form of corneal ulcerative diseases within the domestic animal species.[23] Therefore, a profound

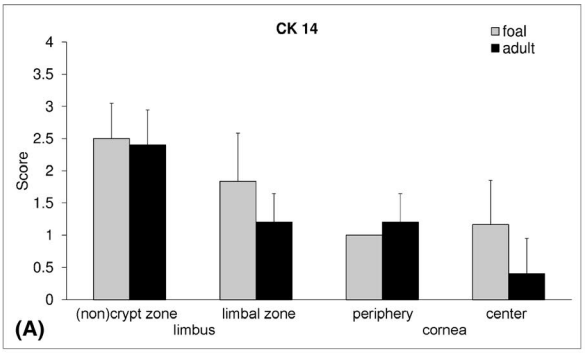
CK 14
foal
adult
Score
4
3.5
3
2.5
2
1.5
1
0.5
0
(non)crypt zone
limbal zone
periphery
center
limbus
cornea
(A)

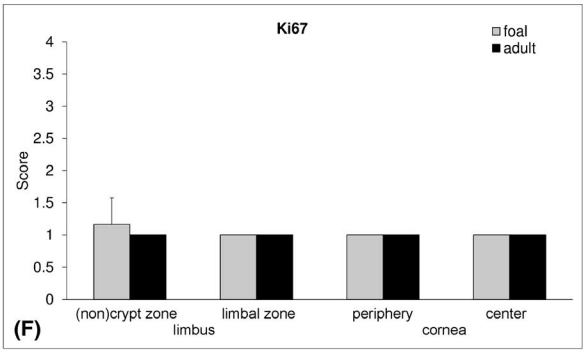
Ki67
foal
adult
Score
4
3.5
3
2.5
2
1.5
1
0.5
0
(non)crypt zone
limbal zone
periphery
center
limbus
cornea
(F)

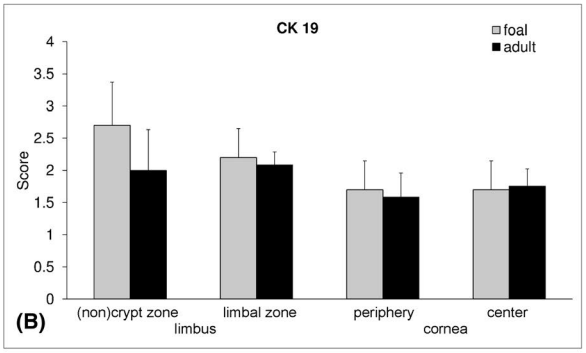
CK 19
foal
adult
Score
4
3.5
3
2.5
2
1.5
1
0.5
0
(non)crypt zone
limbal zone
periphery
center
limbus
cornea
(B)

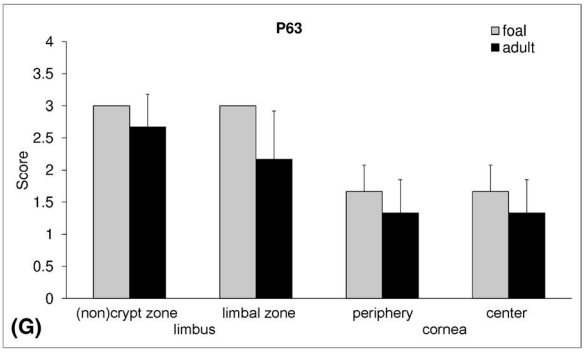
P63
foal
adult
Score
4
3.5
3
2.5
2
1.5
1
0.5
0
(non)crypt zone
limbal zone
periphery
center
limbus
cornea
(G)

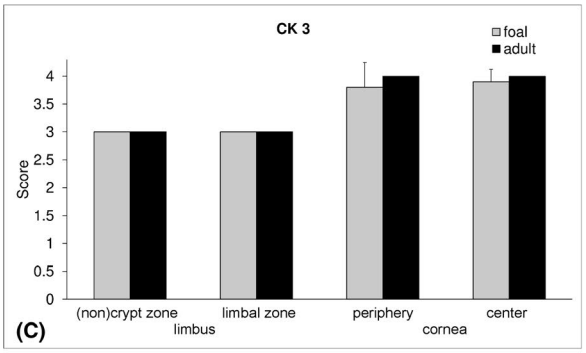
CK 3
foal
adult
Score
4
3.5
3
2.5
2
1.5
1
0.5
0
(non)crypt zone
limbal zone
periphery
center
limbus
cornea
(C)

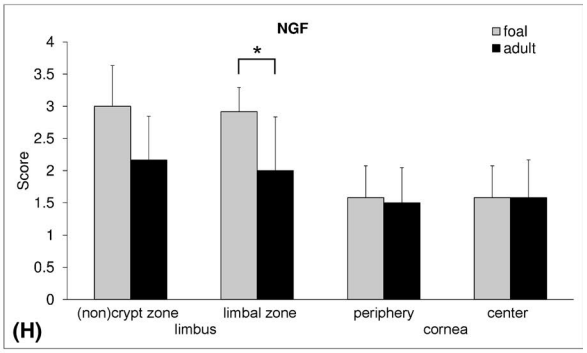
NGF
*
foal
adult
Score
4
3.5
3
2.5
2
1.5
1
0.5
0
(non)crypt zone
limbal zone
periphery
center
limbus
cornea
(H)

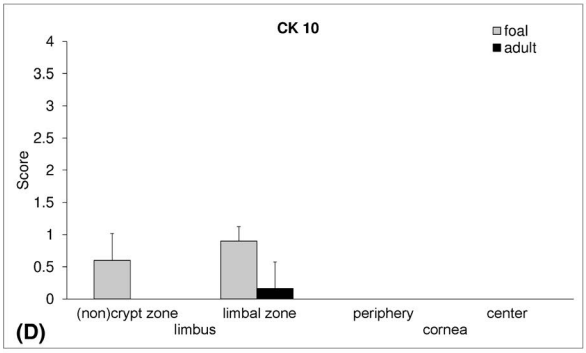
CK 10
foal
adult
Score
4
3.5
3
2.5
2
1.5
1
0.5
0
(non)crypt zone
limbal zone
periphery
center
limbus
cornea
(D)

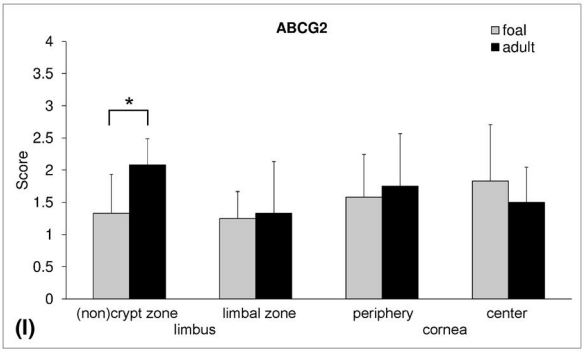
ABCG2
*
foal
adult
Score
4
3.5
3
2.5
2
1.5
1
0.5
0
(non)crypt zone
limbal zone
periphery
center
limbus
cornea
(I)

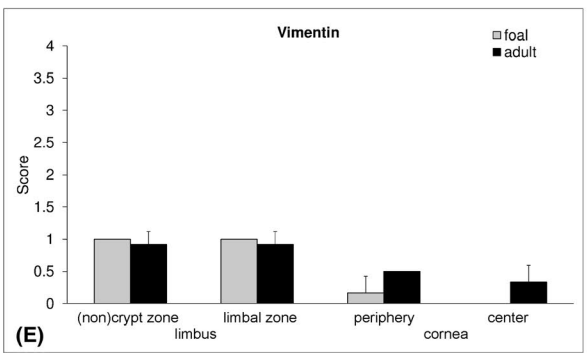
Vimentin
foal
adult
Score
4
3.5
3
2.5
2
1.5
1
0.5
0
(non)crypt zone
limbal zone
periphery
center
limbus
cornea
(E)

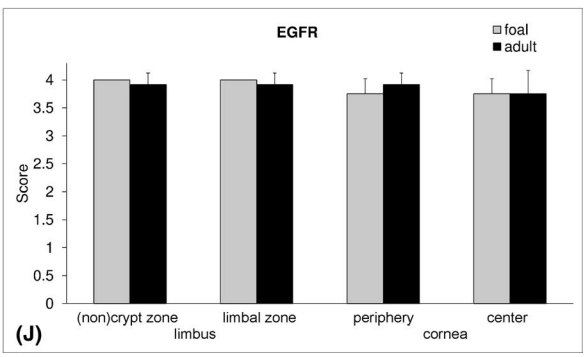
EGFR
foal
adult
Score
4
3.5
3
2.5
2
1.5
1
0.5
0
(non)crypt zone
limbal zone
periphery
center
limbus
cornea
(J)

FIGURE 4 Semiquantitative analysis of immunohistochemical staining for cytoskeletal proteins, proliferation, differentiation, and stem cell markers. CK 14, p63, and NGF showed a gradual decrease from crypt to center. Statistically significant age differences (*, $P < 0.05$) were detected in the limbal zone for NGF and in the crypt/noncrypt zone for ABCG2. Bars represent mean values from six horses of both age groups and whiskers represent SD.

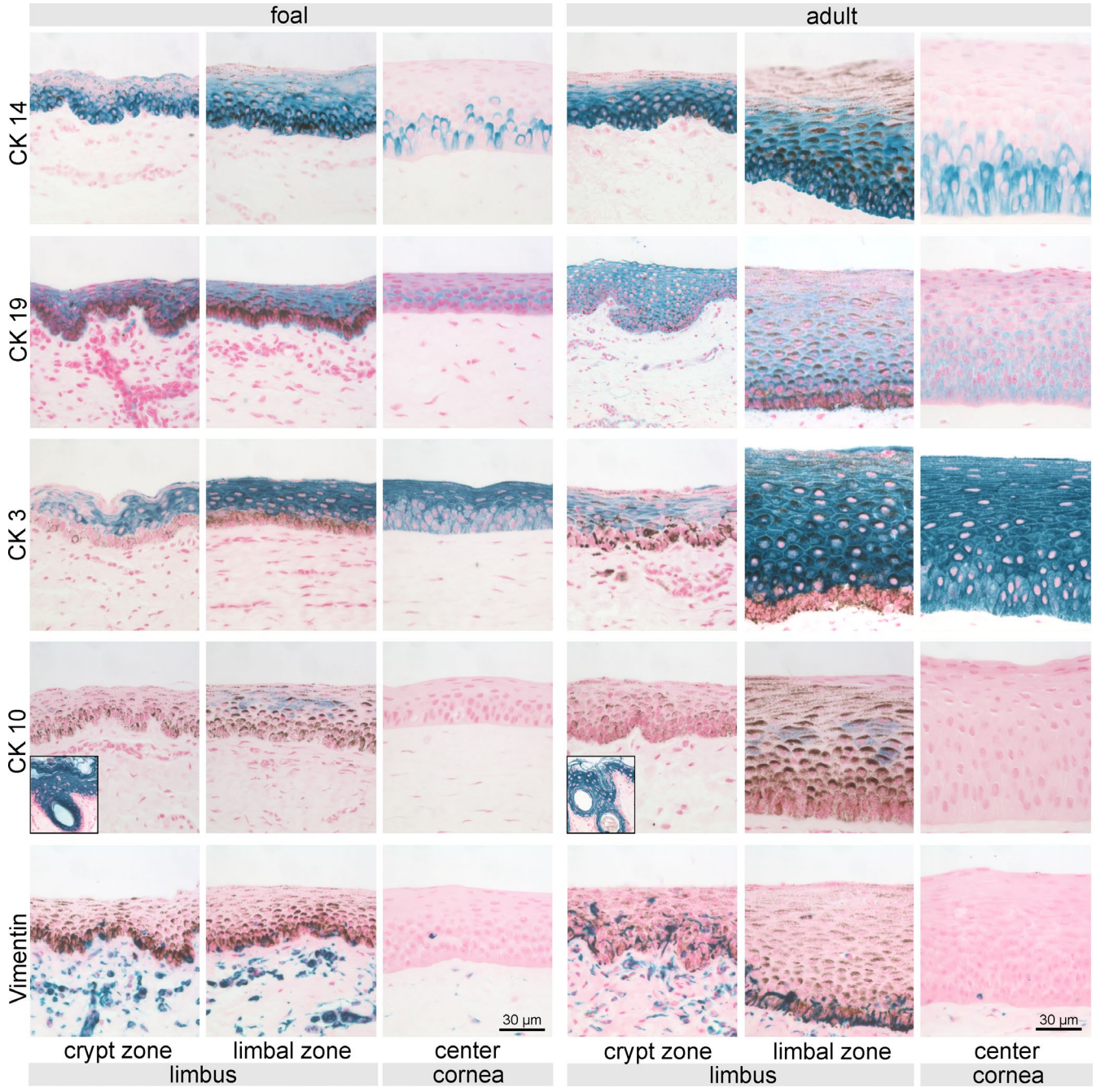

FIGURE 5 Immunohistochemical staining of intermediate filaments CK 14, CK 19, CK 3, CK 10, and vimentin. Representative pictures of crypts, limbus, and central corneal epithelium (and skin used as positive control for CK 10, see inserts) are shown for both foals (left panels) and adult horses (right panels). Potential stem cell marker CK 14 was present in every examined region with decreasing frequency toward the center. Cornea-specific differentiation marker CK 3 was generally present throughout the superficial and intermediate layer, absent in the most basal layer of crypt and limbal epithelium and showed decreased staining intensity in the basal layer of the peripheral and central corneal epithelium. Scale bar =30 µm

histological knowledge of the physiological condition of corneal epithelium is indispensable for a better understanding of mechanisms underlying corneal wound healing, for diagnostic evaluations of pathological corneal alterations and neoplastic changes as well as for the development of modern therapeutic strategies such as SC therapies.

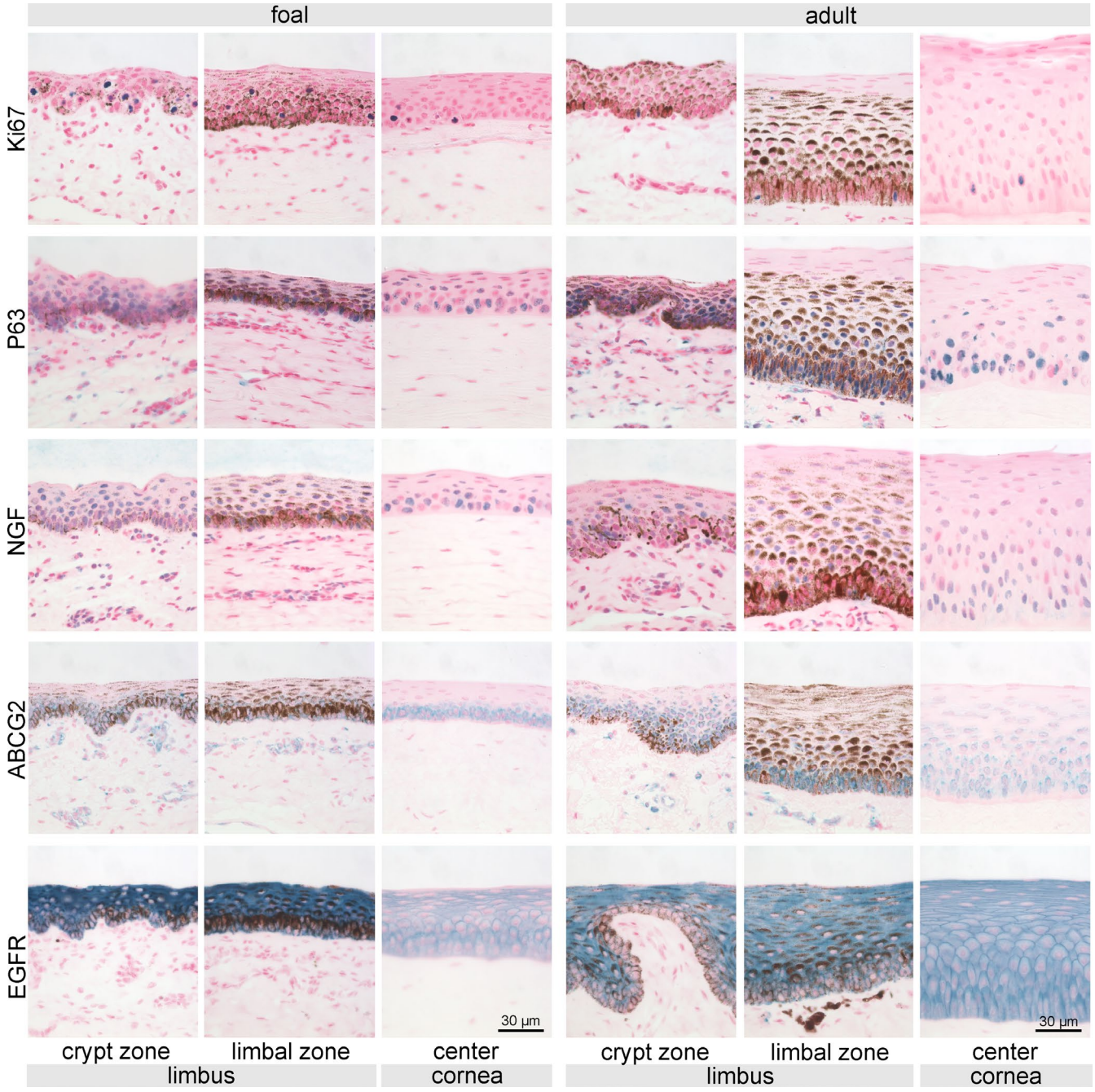

FIGURE 6 Immunohistochemical staining of proposed SC-associated markers Ki67, p63, NGF, ABCG2, and EGFR. Representative pictures of crypts, limbus, and central corneal epithelium are shown for both foals (left panels) and adult horses (right panels). Potential stem cell markers (p63, NGF, and ABCG2) were present in every examined region with decreasing frequency toward the center. Scale bar =30 µm

In accordance with the observations of Patruno et al,[7] we consistently demonstrated the presence of crypts within the limbus in DV sections. These epithelial undulations create an enlarged epithelial surface to accommodate an increased number of cells, such as SCs and melanocytes, and furthermore protect from injuries and the effects of shear forces.[24,25] Therefore, the presence of crypts in horses should be taken into consideration during diagnostic routine and systematic investigations of the corneo-scleral junction in the total circumference in different direction of sectioning are needed in order to further clarify the precise micromorphology and extension of the crypts. The epithelial height and the number of cell layers were consistent with results from the literature in adult horses.[5,9] The differences in the epithelial height between foals and adults are caused by a reduced number of cell layers in the basal and intermediate layer in foals.

Our results clearly showed three distinct layers for the central and peripheral equine cornea: a superficial, an intermediate, and a basal layer supporting the division of Nautscher et al.[5] We further agree with them that the superficial and intermediate layers are composed of a stratified epithelium. Detailed analysis of the basal layer in adult horses, however, revealed three cell types of different height classifying this layer as a pseudostratified epithelium. Our finding of nuclei being located at different levels within the basal layer could explain the result of Ledbetter and Scarlett,[9] who described via in vivo confocal microscopy the highest cell density but only occasionally visible nuclei in the one cell layer directly above the basement membrane (ie, which they termed basal layer). Large and elongated basal cells have also been described in the corneal epithelium of camels and were interpreted as a morphological reflection of environmental conditions to protect stroma from dehydration.[2] Despite the considerably higher equine corneal epithelium compared to other species, damage of the corneal epithelium may affect the basement membrane sooner than expected due to the pseudostratified arrangement of the basal layer. Therefore, these structural epithelial characteristics should be taken into account during surgical procedures as well as for diagnostic and prognostic evaluations.

The integrity of the corneal epithelium which is maintained by intercellular junctional proteins is crucial for corneal health and downregulation of these proteins are well-known indicators for pathological conditions such as epithelial-mesenchymal transition during tumorgenesis.[26] The cell adhesion proteins E-cadherin and β-catenin were seen throughout the entire height of the cornea as well as in all examined zones in our study, which has also been reported for the corneal epithelium of rabbits and dogs.[10,27] Interestingly, this is in contrast to the human cornea, where the E-cadherin/β-catenin complex has been described in suprabasal epithelial cell layers and in less differentiated limbal cells.[18,21,28] Therefore, species-specific differences seem to exist for the localization of the E-cadherin/β-catenin complex in the corneal and limbal epithelium.

In this study, the cell communication protein Cx43 was expressed in basal cells of all zones. Detailed analysis of this protein is lacking in veterinary corneal research and conflicting results have been reported for humans. While some authors demonstrated Cx43 expression also in crypt-associated structures in the human limbus,[12,15] others have described a lack of Cx43 immunolocalization in limbal basal cells as a characteristic to identify SCs.[11,29,30] Based on our results, we suggest that Cx43 cannot be interpreted as a negative marker for the detection of corneal SCs in horses.

Our findings for the localization of TJP1 (also known as ZO1) agree well with the results of previous studies on corneal epithelium of humans and rabbits.[13,31,32] Two immunolocalizations and thus two functions have been described for ZO1 within the corneal epithelium: ZO1 expression at the lateral boundary of apical cells was determined as tight junctions.[31,32] Focal ZO1 expression in basal and suprabasal cells have been associated with the protein paxillin suggesting that the cell adhesions at these sites were dynamic and without barrier function.[13,31,32] Therefore, we suggest that basal TJP1 expression resemble such dynamic adhesion complexes.

CKs have been used as markers for cornea-specific epithelial differentiation and SCs characterization. Our results of CK 14, CK 19, and CK 3 expression in the equine cornea are in accordance with previous research on cornea.[3,11,21,33,34] In the equine corneal epithelium, CK 14 and 19 expression reflect epithelial differentiation but are no suitable marker for exclusive SC detection. Based on our as well as previously reported results, the combination of positive CK 14 expression with the absence of CK 3 expression is appropriate to identify SCs,[3,21] and we therefore conclude that SCs in the equine cornea are exclusively located in the limbus. In the peripheral and central cornea, however, CK 14 positive cells displayed positive, though weaker CK 3 expression representing TACs in agreement with previous interpretations.[11]Although vimentin has been interpreted as additional SC marker,[12,15] we found vimentin as well as CK 10 not suitable for identification of SCs or TACs. In our study, vimentin-positive cells more likely resemble melanocytes and migrating immune cells based on their morphology and distribution. Proliferation as sign for potential regeneration capacity has been detected predominantly in suprabasal cells in the limbus in accordance with human results.[35] In equine juvenile corneal epithelium higher numbers of actively cycling cells were also located more superficially illustrating the developmental stage with proliferating TACs.

As a member of the p53 tumor-suppressor gene family, the transcription factor p63 is an essential parameter in the development of a stratified epithelium and is also associated with proliferative capacity.[36,37] ABCG2 belongs to the superfamily of the ATP-binding cassette (ABC) efflux transporter and plays a crucial role during tissue protection and drug disposition.[38,39] NGF is a member of the neurotrophin family and has been reported to have effects on SCs outside the nervous system.[40] Our results revealed similar distribution patterns for these putative SC markers. Of these markers, p63 has been consistently found in basal and suprabasal cells in the limbus of horses,[3,7] goats,[41] rabbits,[42,43] dogs,[4] humans,[17] and lab animals.[44] Conflicting results, however, have been reported for the center of the cornea: no p63 expression has been detected in rabbits,[42,43] only sporadically in suprabasal cells of goats[41] and, consistent with our results, positive basal and suprabasal cells have been found throughout the corneal epithelium in humans,[17] dogs,[4] and horses.[34] Our results support the interpretation of Schlötzer-Schrehardt and Kruse,[11] that basal p63 positivity may represent cells in proliferative state

such as TACs and only include the corneal epithelial SC population.

In accordance with the human cornea,[22] we found NGF in basal cells of crypt/noncrypt, limbal, and peripheral zones, however, additional positive cells were present in the center. Consistent results have been described for ABCG2 expression of basal and suprabasal cells of limbus of humans,[17] dogs,[4] and rabbits.[43] However, conflicting results have been reported regarding the central cornea, since ABCG2 was shown to be absent in dogs[4] and rabbits,[43] but in agreement with our findings positive cells have been found in humans.[17] Therefore, a conclusion corresponding to p63 can be drawn for NGF and ABCG2. Although a higher expression of EGFR in basal limbal epithelial cells in humans has been reported and interpreted as characteristic for SCs,[21] we found equally strong expression for EGFR in the total height of crypt/noncrypt and limbal epithelium. Therefore, we conclude that EGFR is not a suitable marker to identify SCs and TACs in horses.

This study presents a comprehensive evaluation of the equine cornea epithelium, showing the presence of crypts as potential stem cell niche. SCs in the equine cornea are located in the basal layer of the limbus indicated by the exclusive absence of CK 3. CK 14, p63, NGF, and ABCG2 were identified as relevant markers of cells with potential regenerative capacity, such as TACs. The pseudostratified arrangement of the basal cell layer in adult horses was a unique finding.

ACKNOWLEDGMENTS

The authors would like to acknowledge the colleagues of the pathological dissection department for their help in obtaining corneal samples. Furthermore, the authors thank Brigitte Machac, Dipl.-Ing. (FH) Claudia Höchsmann and Mag. rer.nat. Waltraud Tschulenk for technical support and Dr. Alexander Tichy for statistical advice.

REFERENCES

1. Majo F, Rochat A, Nicolas M, et al. Oligopotent stem cells are distributed throughout the mammalian ocular surface. *Nature*. 2008;456(7219):250-254.
2. Almubrad T, Akhtar S. Ultrastructure features of camel cornea-collagen fibril and proteoglycans. *Vet Ophthalmol*. 2012;15:36-41.
3. Moriyama H, Kasashima Y, Kuwano A, et al. Anatomical location and culture of equine corneal epithelial stem cells. *Vet Ophthalmol*. 2014;17(2):106-112.
4. Morita M, Fujita N, Takahashi A, et al. Evaluation of ABCG2 and p63 expression in canine cornea and cultivated corneal epithelial cells. *Vet Ophthalmol*. 2015;18(1):59-68.
5. Nautscher N, Bauer A, Steffl M, et al. Comparative morphological evaluation of domestic animal cornea. *Vet Ophthalmol*. 2016;19(4):297-304.
6. Sanchez RF, Daniels JT. Mini-review: limbal stem cells deficiency in companion animals: time to give something back? *Curr Eye Res*. 2016;41(4):425-432.
7. Patruno M, Perazzi A, Martinello T, et al. Morphological description of limbal epithelium: searching for stem cells crypts in the dog, cat, pig, cow, sheep and horse. *Vet Res Commun*. 2017;41(2):169-173.
8. Patruno M, Perazzi A, Martinello T, et al. Investigations of the corneal epithelium in Veterinary Medicine: State of the art on corneal stem cells found in different mammalian species and their putative application. *Res Vet Sci*. 2018;118:502-507.
9. Ledbetter EC, Scarlett JM. In vivo confocal microscopy of the normal equine cornea and limbus. *Vet Ophthalmol*. 2009;12(Suppl. 1):57-64.
10. Bardag-Gorce F, Hoft RH, Wood A, et al. The role of E-Cadherin in maintaining the barrier function of corneal epithelium after treatment with cultured autologous oral mucosa epithelial cell sheet grafts for limbal stem deficiency. *J Ophthalmol* 2016;2016: 1-13. art. no. 4805986.
11. Schlötzer-Schrehardt U, Kruse FE. Identification and characterization of limbal stem cells. *Exp Eye Res*. 2005;81(3):247-264.
12. Nubile M, Curcio C, Dua HS, et al. Pathological changes of the anatomical structure and markers of the limbal stem cell niche due to inflammation. *Mol Vis*. 2013;19:516-525.
13. Wang Y, Chen M, Wolosin JM. ZO-1 in corneal epithelium; stratal distribution and synthesis induction by outer cell removal. *Exp Eye Res*. 1993;57(3):283-292.
14. Townsend WM. The limbal palisades of Vogt. *Trans Am Ophthalmol Soc*. 1991;89:721-756.
15. Shanmuganathan VA, Foster T, Kulkarni BB, et al. Morphological characteristics of the limbal epithelial crypt. *Br J Ophthalmol*. 2007;91(4):514-519.
16. Shortt AJ, Secker GA, Munro PM, et al. Characterization of the limbal epithelial stem cell niche: novel imaging techniques permit in vivo observation and targeted biopsy of limbal epithelial stem cells. *Stem Cells*. 2007;25(6):1402-1409.
17. Chang CY, Green CR, McGhee CN, et al. Acute wound healing in the human central corneal epithelium appears to be independent of limbal stem cell influence. *Invest Ophthalmol Vis Sci*. 2008;49(12):5279-5286.
18. Lin J, Yoon KC, Zhang L, et al. A native like corneal construct using donor corneal stroma for tissue engineering. *PLoS One*. 2012;7(11):e49571.
19. Magin TM, Vijayaraj P, Leube RE. Structural and regulatory functions of keratins. *Exp Cell Res*. 2007;313:2021-2032.
20. Geburek F, Ohnesorge B, Deegen E, et al. Alterations of epidermal proliferation and cytokeratin expression in skin biopsies from heavy draught horses with chronic pastern dermatitis. *Vet Dermatol*. 2005;16:373-384.
21. Chen Z, de Paiva CS, Luo L, et al. Characterization of putative stem cell phenotype in human limbal epithelia. *Stem Cells*. 2004;22(3):355-366.
22. Qi H, Li DQ, Shine HD, et al. Nerve growth factor and its receptor TrkA serve as potential markers for human corneal epithelial progenitor cells. *Exp Eye Res*. 2008;86(1):34-40.
23. Brooks DE, Wolf ED. Ocular trauma in the horse. *Equine Vet J*. 1983;15(S2):141-146.
24. Gipson IK. The epithelial basement membrane zone of the limbus. *Eye*. 1989;3:132-140.

25. Yoon JJ, Ismail S, Sherwin T. Limbal stem cells: Central concepts of corneal epithelial homeostasis. *World J Stem Cells*. 2014;6(4):391-403.
26. Chen A, Beetham H, Black MA, et al. E-cadherin loss alters cytoskeletal organization and adhesion in non-malignant breast cells but is insufficient to induce an epithelial-mesenchymal transition. *BMC Cancer*. 2014;14(1):552.
27. Chandler HL, Colitz CM, Lu P, et al. The role of the slug transcription factor in cell migration during corneal re-epithelialization in the dog. *Exp Eye Res*. 2007;84(3):400-411.
28. Lu R, Bian F, Zhang X, et al. The β-catenin/Tcf4/survivin signaling maintains a less differentiated phenotype and high proliferative capacity of human corneal epithelial progenitor cells. *Int J Biochem Cell Biol*. 2011;43(5):751-759.
29. Matic M, Petrov IN, Chen S, et al. Stem cells of the corneal epithelium lack connexins and metabolite transfer capacity. *Differentiation*. 1997;61(4):251-260.
30. Chen Z, Evans WH, Pflugfelder SC, et al. Gap junction protein connexin 43 serves as a negative marker for a stem cell-containing population of human limbal epithelial cells. *Stem Cells*. 2006;24(5):1265-1273.
31. Sugrue SP, Zieske JD. ZO1 in corneal epithelium: association to the zonula occludens and adherens junctions. *Exp Eye Res*. 1997;64(1):11-20.
32. Ban Y, Dota A, Cooper LJ, et al. Tight junction-related protein expression and distribution in human corneal epithelium. *Exp Eye Res*. 2003;76(6):663-669.
33. Chen B, Mi S, Wright B, et al. Investigation of K14/K5 as a stem cell marker in the limbal region of the bovine cornea. *PLoS ONE*. 2010;5(10):e13192.
34. Linardi RL, Megee SO, Mainardi SR, et al. Expression and localization of epithelial stem cell and differentiation markers in equine skin, eye and hoof. *Vet Dermatol*. 2015;26(4):213-e47.
35. Joyce NC, Meklir B, Joyce SJ, et al. Cell cycle protein expression and proliferative status in human corneal cells. *Invest Ophthalmol Vis Sci*. 1996;37(4):645-655.
36. Yang A, Kaghad M, Wang Y, et al. p63, a p53 homolog at 3q27-29, encodes multiple products with transactivating, death-inducing, and dominant-negative activities. *Mol Cell*. 1998;2:305-316.
37. Parsa R, Yang A, McKeon F, et al. Association of p63 with proliferative potential in normal and neoplastic human keratinocytes. *J Invest Dermatol*. 1999;113:1099-1105.
38. Mao Q, Unadkat JD. Role of the breast cancer resistance protein (ABCG2) in drug transport. *AAPS J*. 2005;7:E118-E133.
39. Robey RW, To KK, Polgar O, et al. ABCG2: a perspective. *Adv Drug Deliv Rev*. 2009;61:3-13.
40. Daiko H, Isohata N, Sano M, et al. Molecular profiles of the mouse postnatal development of the esophageal epithelium showing delayed growth start. *Int J Mol Med*. 2006;18:1057-1066.
41. Yin JQ, Liu WQ, Liu C, et al. Reconstruction of damaged corneal epithelium using Venus-labeled limbal epithelial stem cells and tracking of surviving donor cells. *Exp Eye Res*. 2013;115:246-54.
42. Tananuvat N, Bumroongkit K, Tocharusa C, et al. Limbal stem cell and oral mucosal epithelial transplantation from ex vivo cultivation in LSCD-induced rabbits: histology and immunologic study of the transplant epithelial sheet. *Int Ophthalmol*. 2017;37(6):1289-1298.
43. Yeh SI, Ho TC, Chen SL, et al. Pigment epithelial-derived factor peptide regenerated limbus serves as regeneration source for limbal regeneration in rabbit limbal deficiency. *Invest Ophthalmol Vis Sci*. 2016;57(6):2629-36.
44. Hsueh YJ, Wang DY, Cheng CC, et al. Age-related expressions of p63 and other keratinocyte stem cell markers in rat cornea. *J Biomed Sci*. 2004;11(5):641-51.

How to cite this article: Kammergruber E, Rahn C, Nell B, Gabner S, Egerbacher M. Morphological and immunohistochemical characteristics of the equine corneal epithelium. *Vet Ophthalmol*. 2019;22:778–790. https://doi.org/10.1111/vop.12651